# MONOLITHIC MULTICHANNEL GAN LED ARRAYS FOR OPTOGENETICS

By

Wasif Afsari Khan

A THESIS

Submitted to
Michigan State University
in partial fulfillment of the requirements
for the degree of

Electrical Engineering – Master of Science

2016

# ABSTRACT

## MONOLITHIC MULTICHANNEL GAN LED ARRAYS FOR OPTOGENETICS

By

Wasif Afsari Khan

Establishment of a reliable bi directional communication channel between the nervous system of a freely behaving vertebrate and the external environment is important for the treatment of neurological diseases and events like spinal cord injury, stroke and traumatic major amputations. Optogenetics, which uses light stimulation to control the excitation and inhibition of action potentials in genetically modified neurons. However, conventional methods like tethered optical fiber impedes the subject from moving freely and poor spatial resolution of other methods limits their functionality. A light-stimulating interface with sufficient light intensity that also allows free behavior of the experiment subject is imperative.

In response to meet these challenges, monolithic multichannel micro LED arrays have been fabricated using less expensive reactive ion etching. These LED arrays could be surgically implanted on the cortex of an animal subject to stimulate light in vivo without hindering the animal's free behavior. Annealing was performed to improve the performance of the LED's. These arrays demonstrated sufficient light intensity that is required for genetically modified neuron activation. The fabricated LED's showed lower heat dissipation, which reduces the risk of impairing the neurons. The results of the RIE etching process, electrical and optical performance of the fabricated LED arrays were also characterized.

# TABLE OF CONTENTS

# LIST OF TABLES

# LIST OF FIGURES

# CHAPTER 1: INTRODUCTION

The combination of genetic and optical methods on living tissue and behaving animals to cause or inhibit events in specific cells is known as optogenetics. The control of cells in living systems has been achieved through the development of the microbial opsin, genetic method for cell type targeting and optical method to guide light through tissues.

The microbial opsin proteins transduce photons into electrical current. Three families of these opsins have found their use in optogenetics. The bacterio-rhodopsins, the halo-rhodopsins (inhibitory) and the channel-rhodopsins (excitatory). The bacteriorhodopsins pump protons out of the cell, the halorphodopsins pump chloride ion into the cell and the channelrhodopsins ensures flow of positive ions through the ion channel pores. With the introduction of fast light of proper intensity and wavelength, these opsins will open the corresponding ion channels in neuron cells to create inhibitory or excitatory behavior.

It is apparent that there is a necessity for a device in optogenetics that can effectively convert electrical energy into light energy. The phenomena of light emission from a solid-state material, by applying an electrical power are known as electroluminescence. Usually in a semiconductor, electroluminescence occurs because of the radiated recombination of charge carriers electron and holes.

Among the light illuminating devices manufactured now a day, the most promising emerging technology is of the light emitting diodes (LED). These semiconductor devices

possess desirable features, along with high efficiency and low power consumption when compared with incandescent lamps or arc lamps. The LEDs are efficient enough to be powered by low voltage batteries and inexpensive switchable power supplies. The diverse spectral output offered by LEDs makes it possible to select an individual diode light source to supply the optimum excitation wavelength band for spanning the ultraviolet, visible, and near-infrared regions.

GaN LEDs, when powered with adequate voltage, generates blue light at the wavelength of 450-495 nm. This wavelength is sufficient for the activation of channelrhodopsin, which is maximally excited at 470nm.

An interesting area to study optogenetics is the visual cortex of the brain. In order to effectively record action potentials from the various neurons of the visual cortex, a device with an array of LED is desired. Current approach is to make interconnections on a biocompatible polymer substrate, and manually assemble individual LED's using low melting temperature solder. A significant improvement to this approach could be made by fabricating arrays of LED monolithically, adding additional components on the LED's instead of manual assembly, and by having a higher spatial resolution resulting in enabling multichannel recording. Further advancements could be made by coupling waveguides for precise light delivery or attaching micro lens on the LED to reduce invasive procedures while having precise light transport. Transferring the monolithically fabricated arrays on a flexible substrate also has the possibility to increase the flexibility of the overall device.

This thesis presents a fabrication process of monolithic GaN LED arrays by reactive ion etching to be used in optogenetics- specifically in activating the sensory photoreceptor channelrhodopsin. The electrical and optical characteristics were also illustrated in this thesis.

In this work, reactive ion etching was used to etch the GaN epitaxial layer and form a p-n junction. Etch rates were found under different RF power conditions. Also changes on the etch rates for different substrate condition were studied. Temperature effect during the RIE etching was studied for different etch rates. To create an ohmic contact for the n-GaN and p-GaN, Ti/Al/Ni/Au and Ni/Au was used respectively. The I-V characteristics for the fabricated LED's were illustrated and analyzed. Optical power for the LED at different electrical power was shown. Heat generation by the LED's is shown as infrared images. Lastly, annealing effect on the metal contacts was studied for the I-V characteristics and optical power.

This thesis is structured as follows: chapter 2 will begin with a review of the concept of optogenetics, its relationship with GaN LED arrays and current technologies used in optogenetics for light stimulation. Chapter 3 will discuss about the fabrication process of the monolithic GaN LED arrays. In Chapter 4, analysis of the electrical, thermal and optical properties of the fabricated arrays will be discussed. Statistical analysis on the measured data will be represented in this chapter. Chapter 5 is the conclusion and future outlook. A brief conclusion reviews the achievements of this work and challenges the remaining. The outlook section discusses the work necessary to develop a fully functional device for

optogenetics, which will be able to stimulate light and record data from specific neurons based on the arrays discussed in chapter 3 and 4. Also will be discussed the different directions this work could take in the future.

# CHAPTER 2: BACKGROUND

## 2.1 OPTOGENETICS

Optogenetics is a biological technique which involves the use of light to control cells in living tissue, typically neurons, that have been genetically modified to express light-sensitive ion channels. It is a neuromodulation method employed in neuroscience that uses a combination of techniques from optics and genetics to control and monitor the activities of individual neurons in living tissue—even within freely-moving animals—and to precisely measure the effects of those manipulations in real-time. The key reagents used in optogenetics are light-sensitive proteins.

## 2.2 OPTOGENETICS AND ELECTRICAL STIMULATION

If we consider two equivalent experiments, one using light sensitive protein (ChR2) injected into the brain tissue-the protein being activated by light while the other using an electrical micro stimulator/electrode to provide electrical stimulation. Both of these stimulations will lead to the generation of action potentials. In the optogenetic experiment, the targeted region and the cells will be selectively activated, referring to the activation of synapses, cells and circuits connected downstream of the targeted neuron. While the stimulation by the microstimulators might first lead to spikes in diverse local and afferent, and then pass onto the axonal fibers.

## 2.3 IMPORTANCE OF OPTOGENETICS

As a matter of fact, powerful therapeutic strategies in clinical neuroscience and remarkable information in neuroscience were obtained through the temporal precision of the

extracellular electrodes (electrical stimulation). A massive amount of information was accumulated for the treatment of movement disorders by the surgically implanted electrodes into deep brain structures. A similar revolution might also take place in psychiatry for alleviation of many neuropsychiatric conditions. However, there are difficulties that limit the application of electrodes to free movement of behaving animals and human beings. The extracellular electrodes have limited control of target region and cellular specificity. They are unable to target a specific class of neurons within a heterogeneously populated tissue. In fact, these electrodes activate all classes of excitatory and inhibitory neurons and fibers of passage in the stimulated area.

## 2.4 NEED FOR OPTOGENETICS

Francis Crick at 1979 mentioned the fact that electrodes cannot readily distinguish different cell types due to the complex mammalian brain. According to his suggestion, there was the need to precisely control activity in one cell type while leaving the others unaltered. The speculation was towards light-whether it might be a relevant control tool

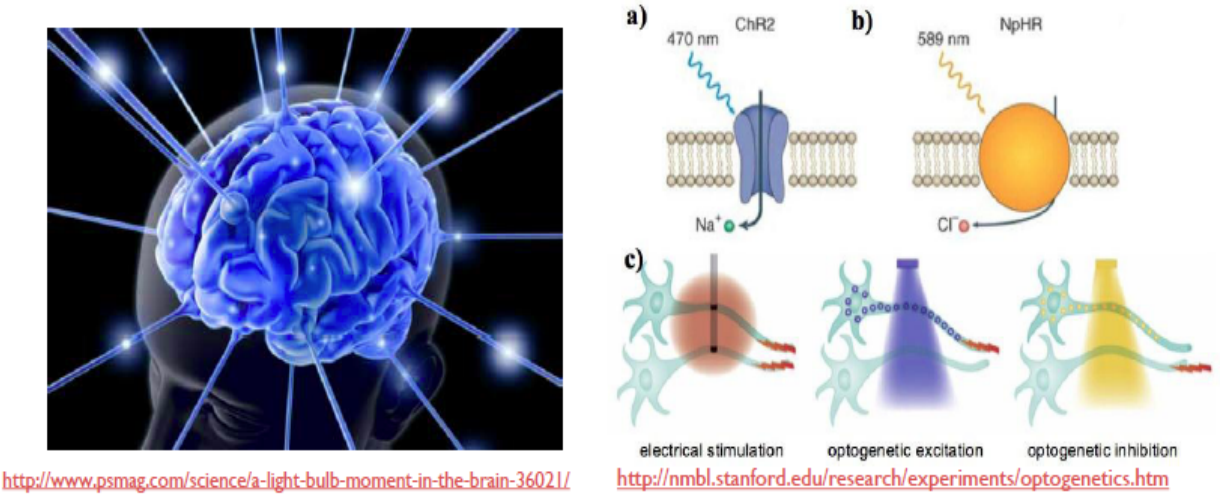


Figure 2-1. Electrical and optogenetic stimulation on neurons

[3]. The use of optogenetic tools eliminates the limitations of the electrodes and allows control on the cells of the targeted region.

## 2.5 OPTOGENETIC ACTUATORS

Spatially-precise neuronal control is achieved using optogenetic actuators like channel-rhodopsin, halo-rhodopsin, and archae-rhodopsin, while temporally-precise recordings can be made with the help of optogenetic sensors for calcium (Aequorin, Cameleon, GCaMP), chloride (Clomeleon) or membrane voltage.

The interest of this thesis lies on the spatial neuronal control. The requirement for spatial control are as follows i) targeting specific cells by controlled tools ii) precise and sufficient light delivery iii) integration of the optical control with compatible readouts [2].

## 2.6 HISTORY OF OPTOGENETICS

For a couple of decades, it was known by the microbiologists that the flow of ions through the plasma membrane is regulated by some micro organisms by producing light gated proteins. In 1971, the functions of bacterio-rhodopsin as an ion pump was discovered [5], followed by the discovery of halo-rhodopsin in 1977 [6] and channel-rhodopsin in 2002 [7].

However, it took the neuro-scientists more than 30 years to introduce this production of light gated proteins for neuroscience studies [3]. In 2005, it was reported that the

introduction of a microbial opsin gene without any other chemicals or components, the neurons become responsive to light [4].

## 2.7 OPSIN GENES

The first opsin gene to be identified was the bacteriorhodopsin. Under low oxygen conditions, it pumped protons from the cytoplasm to the extracellular medium to drive a proton motive force to drive ATP synthesis [8] in order to serve as an alternate energy production system. The halorhodopsin is a light activated chloride pump [9], and the direction of pumping is from the extracellular to the intracellular space causing inhibition. For Channelrhodopsin, the activation was dominated by the inflow of cations [10], which causes depolarization of the membrane potential, thus causing activation.

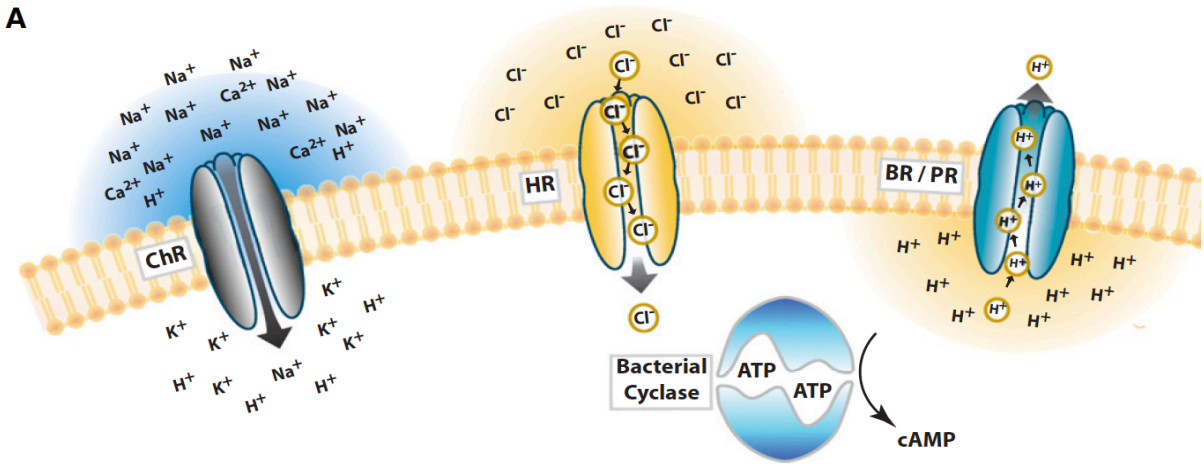


Figure 2-2. Direction of ion flow through ion channels for different opsin genes [2]

The peak activation wavelength of the bacteriorhodopsin is at 566nm [13], while the halorhodopsin and the channelrhodopsins have their peak activation wavelength at

590nm, [12] which corresponds to yellow light and 470nm, [11] which corresponds to blue light respectively.

## 2.8 CHANNELRHODOPSINE AND OPTICAL STIMULATION

The most commonly used approach to date is the viral transduction of channelrhodopsin (ChR2) in the brain tissue. ChR2 expressing viral vectors can be delivered to the targeted brain region by injecting with efficacy and minimal tissue damage. Adeno-associated viruses provide extensive spatial spread and high expression levels [14]. The successful use of optogenetic techniques relies on the sufficient expression levels of the light activated ion channels, which essentially requires sufficient intensity of the specific wavelength light. Studies were performed using laser diodes coupled with optical fibers to stimulate light onto behaving animals. This approach of light delivery ensures sufficient intensity and generated remarkable results [15]. However, coupling the optical fiber with the cortex requires invasive surgery and limits the free movement of the animal. An alternative approach to solve this issue is the incorporation of light emitting diodes as the optical source.

## 2.9 NECESSITY OF BLUE LIGHT EMITTING LED

The necessity for an LED having the properties of emitting blue light at sufficient intensity leads to gallium nitride based light emitting diodes. Gallium nitride (GaN) is a binary III/V direct bandgap semiconductor commonly used in bright light-emitting diodes . The compound is a very hard material that has a Wurtzite crystal structure. Its wide band gap of 3.4 eV affords it special properties for applications in optoelectronic, high-power and

high-frequency devices. Wide bandgap (AlGaIn)N-based heterostructures were widely studied for the optimization of optoelectronic devices that required light emission in the spectral range of UV-blue-green light. These LED's can work as primary light sources to excite organic or inorganic materials for subsequent photon emission at lower energies. GaN is non-toxic and biocompatible, which makes the LED's fabricated using GaN a promising tool for optogenetics.

## 2.10 DRY ETCHING OF GAN

In order to reduce lattice mismatch and difficulties in the growth of bulk material, metalorganic-chemical-vapor-deposition (MOCVD) grown GaN layers are grown heteroepitaxially onto dissimilar substrates, such as sapphire and SiC. The sapphire is the most commonly used substrate because of its relatively low cost. However, due to its high chemical inertness, it was found that this wide band gap material is difficult to pattern by wet chemical treatment [16,17]. Although studies indicate that GaN dissolves in hot phosphoric acid [18] and alkalisolution [19] at a very slow rate, achieving a fine pattern transfer is practically not feasible using these etching techniques. The chemical inertness, along with the necessity to decrease dimensions, have led to significant efforts into the investigation of dry etch processing.

The reactive ion etching of GaN was studied using a variety of gases including $SF_6$, $SiCl_4$, $CCl_2F_2$ and $BCl_3$ [19,20]. High Ion bombardment is created in the plasma to break the strong III-N bond and to allow desorption of the etch products from the surface. Gases containing hydrogen- like $CH_4$ [22,23] and HBr [24] have also been used to etch GaN.

Electron cyclotron resonance (ECR)–RIE process was developed for further improvement towards etching GaN. Use of $Cl_2/CH_4$ in the ECR-RIE led to achieve etch rates greater than 100 nm $min^{-1}$ [25].

The implementation of high-density plasma (HDP) is considered to be a remarkable advancement for GaN device fabrication [26, 27] using dry etching. To achieve a high reactive species content along with independent control of the ion energy, HDP processing could be a lucrative option. A subset of HDP, the inductively coupled plasma (ICP) has been commonly used for etching of GaN. Results were reported with high etch rate and anisotropic profiles by using ICP [28] compared to RIE. However, equipment expense and maintenance cost for ICP and ECR-RIE is much higher than a conventional RIE. Not only the expense is a drawback, but studies also report that ICP $Cl_2$/Ar degrades the performance of GaN diodes [29].

Using $Cl_2$ and $BCl_3$ as the reactive gases, ion beam techniques such as reactive ion beam etching [30] (RIBE) or chemically assisted Ar ion beam etching [31,32] (CAIBE) have been implemented to etch GaN. Higher etch rates in the range of 50-100 nm/min was reported. Vertical etch profiles with 0° overcut angle was obtained using CAIBE; by optimizing the Ar beam incidence angle [33] and a high sample temperature [31].

A dry etching using conventional reactive ion etching process of GaN using $SF_6$ was used for the work of this thesis. RIE using $SF_6$ as the reactive gas is popularly used in Si technologies. Although fluoride gases form non volatile $GaF_3$ compounds, which is a disadvantage

compared with the chloride or bromide. However, nitrogen forms volatile $NF_3$ when it reacts with fluorine [21]. Any non-volatile compound formed during the RIE process is also expected to be removed by the accelerated ions [21]. Meanwhile, $SF_6$ is less corrosive and less toxic compared with the chloride and bromide gases, thus provides an advantage from the processes that incorporates chloride and bromides.

## 2.11 METAL CONTACTS FOR LED'S

Improvement of the electrical and optical performance of the fabricated device is extremely dependent on having low-resistance ohmic contacts. A large voltage drop across the GaN/metal contact interface is undesirable and often leads to poor device reliability [34]. The performance could be substantially reduced with a high resistance metal-GaN contact. Hence, development towards achieving a low contact resistance is of great practical importance. Generally, the metal contacts need to provide a low Schottky barrier to form high-quality ohmic contacts to GaN.

There are few approaches to achieve low contact resistivity ohmic contacts. A low barrier height at the metal–semiconductor interface allows thermally energetic electrons to pass over the barrier. The Schottky barrier depends on the work function of the metal selected as the contact metallization [35]. Heavy doping of the semiconductor surface adjacent to the metal, by which the vast majority of ohmic contacts are formed, is achieved either by epitaxial growth, ion implantation and annealing of the surface, or by the deposition of a metal alloy whose subsequent heat treatment effectively dopes the surface of the semiconductor [45].

A low barrier height could be achieved for n-GaN by selecting a metal with a work function close to that of GaN, which has been measured at 4.1 eV [36]. Examples are Ti (Φ = 4.1 eV), Al (Φ =4.28 eV), Ta (Φ = 4.25 eV), and V (Φ = 4.3 eV). For example, Ti-, Al-, or V-based metallization schemes, such as, Ti/Al [37,38], Ti/Al/Ni/Au [39], Ti/Al/$TiAl_3$ [40], Ta/Ti/Ni/Au [41], V/Ti/Au [42] have extensively been studied. For MOCVD-grown p-type GaN, the strategy is to use metals having a large work function. However, due to the absence of materials having a work function larger than p-GaN (Φ=7.5 eV), it is difficult to introduce a low-resistance ohmic contact [43]. The best results could be obtained using the metals with very high work functions. Studies indicate a Ni/Au contact for p-GaN provided better results [44]. The work presented in this thesis follows a Ti/Al/Ni/Au contact for the n-GaN and a Ni/Au metal contact for the p-GaN.

## 2.12 ANNEALING

An annealing process followed by the deposition of contact metals is important to achieve good ohmic properties for both n-type and p-type GaN. Rapid thermal annealing at high temperatures in $N_2$ or Ar ambient is widely used for alloying the Ti/Al contacts [46,47]. Aluminum contacts have reliability issues when exposed to high temperature processing due to the tendency of oxidizing. This lack of reliability also happens when operating under high temperature conditions. Although the oxygen concentration is very low in $N_2$ or Ar ambient under furnace annealing, the aluminum contacts are prone to oxidation above 600 °C.

# CHAPTER 3: FABRICATION PROCESS

GaN based LED epitaxial wafer were obtained from Xiamen Powerway Advanced Material Co., Ltd (PAM-XIAMEN). The growth process for the epistaxis was metal organic chemical vapor deposition (MOCVD). The 2-inch wafer had patterned sapphire as the substrate material. The epitaxial layers and their corresponding thicknesses are given in the following table

Table 3-1. Layer thicknesses of GaN wafer

| Layers | Thickness (um) |
|---|---|
| P-GaN | 0.2 |
| P-AlGaN | 0.03 |
| InGaN/GaN(Active area) | 0.2 |
| n-GaN | 2.5 |
| u-GaN | 3.5 |
| Al2O3 | 430 |

## 3.1 WAFER PREPARATIONS AND MASK METAL DEPOSITION

The wafer was pre cleaned by rinsing with acetone, isopropanol and DI water for 20 seconds. In order to create a metal mask for the RIE process, 500 nm of Copper was deposited using an Edward Auto306 thermal evaporator. A 5nm Titanium layer was deposited before to act as the adhesion layer for copper. Mask design was done using AutoCad.

## 3.2 PATTERN METALS USING PHOTOLITHOGRAPHY

To pattern the deposited metal, photolithography techniques were followed. First the wafer went through the surface dehydration process at 115C for 10 minutes on a hotplate. Then a layer of Shipley S1813 positive photoresist was spin coated at 2000 RPM for 60 seconds on the wafer followed by a soft baking step at 115C for 60 secs. The photoresist was exposed under 120 mJ/cm2 UV light using a AB-M mask aligner. After wards, the exposed photoresist was developed using AZ-352 (AZ351: DI water=1:5) for 40 secs.

A wet etching of the deposited metals were performed after the development of the photoresist. The wafer was submerged in a Ferric chloride solution for 20 secs to etch away the copper. A buffered oxide etch solution containing 49% hydrofluoric acid was used to etch the titanium from the desired places.

## 3.3 WAFER DICING

Next, the wafer was divided into small dice using a MicroAutomation 1006 wafer-dicing saw. The dimensions of the dice were 1 cm X 1.03cm. Alignment marks were designed on each die to allow further fabrication process on the dice. Within the dice, the patterned metal mask for each LED had the dimension of 400X150 um with a separation of 200um in a grid. A 80um diameter circular hole was created in the LED pattern which will be etched up to the n-GaN layer and would serve as the contact.

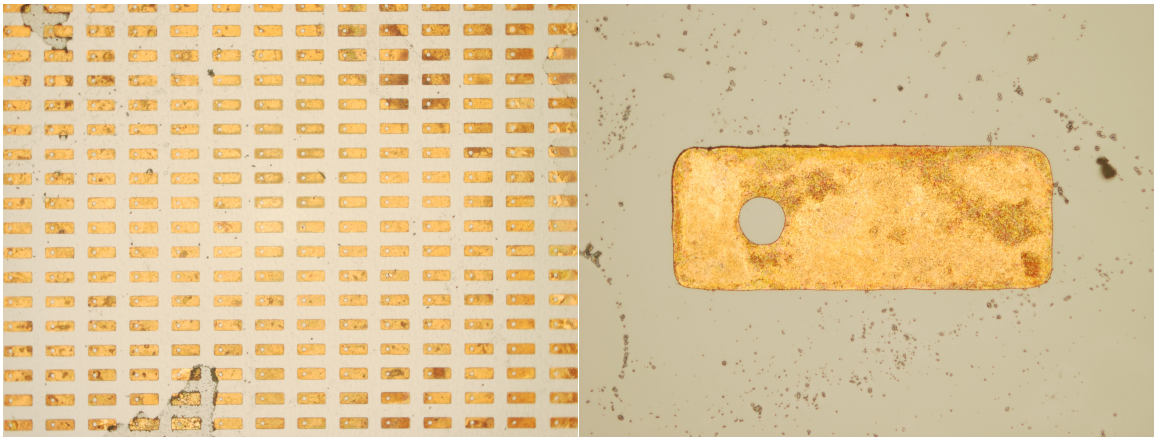

Figure 3-1. Dice and LED chip

## 3.4 REACTIVE ION ETCHING

The LED epitaxial dice were then subjected to reactive ion etching. The dry etching was done using a Nordson March RIE-1701 plasma etching system. Parameters for the plasma etching are given in the table 3-1.

Table 3-2. RIE parameters

| Base Pressure | Process Pressure | Gas Flow | RF Power | Substrate/Carrier Material |
|---|---|---|---|---|
| 15 mT | 200 mT (+- 50mT) | 40 sccm $SF_6$ | 200 W | Sapphire |
| | | | 400W | Silicon |
| | | | 600W | Glass |

Following the anisotropic dry etching of the dice, the metal mask was then removed by using ferric chloride for the copper and buffered oxide etch for the titanium. As the parameters of the dry etching was different for the dice, the corresponding etch depths

were measured after the mask removal by using a Dimension 3100 scanning probe microscope. Etch rates were then calculated from the etch depth and time of etching.

The dry etching process introduces a surface roughness for both the etched n-GaN surface and also the mask covered p-GaN surface due to the formation of pinholes in the copper mask. Surface roughnesses from both of these layers were measured using the scanning probe microscope.

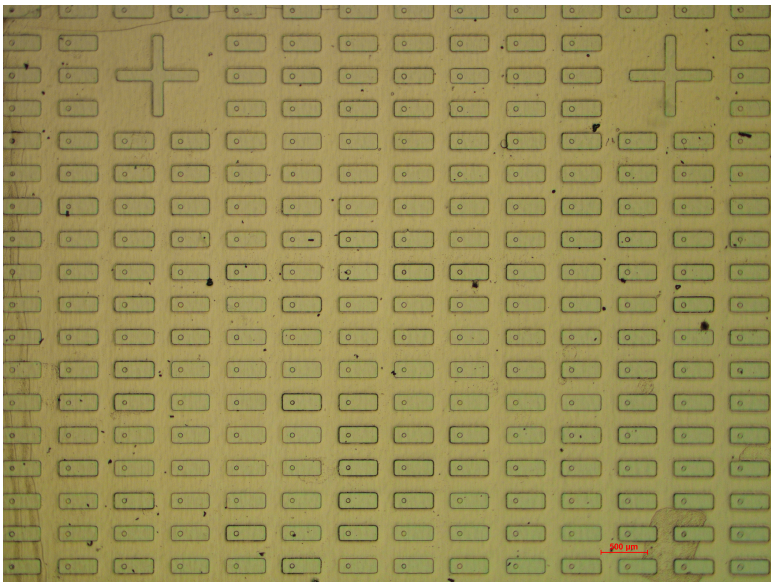

Figure 3-2. Dice after mask removal

## 3.5 OXIDE LAYER DEPOSITION AND PATTERN

A 300A layer of $SiO_2$ was deposited at 300C using a oxford plasmalab 80 plus plasma enhanced chemical vapor deposition machine in order to create an insulation between n-GaN and p-GaN layer contact metals. The oxide layer was later patterned to open up a via of 20 um diameter only at the RIE etched n-GaN surface. The oxide layer was patterned using

Shipley 1813 photoresist exposed at 120 mJ/cm$^2$ with a soft baking step at 115C for 60 secs. The developing time was 40secs in AZ 352 developer. Later on, the insulating oxide was etched by submerging the dice into buffered oxide etch (HF 5%, $NH_4F$ 40%) for 18 secs.

### 3.6 CONTACT METALS DEPOSITION AND PATTERN

The n-GaN and p-GaN contacts needed multiple metals to be deposited and patterned. A conventional wet etching, in this circumstance, involves multiple chemicals for etching different metals. Finding a chemical, which is only selective to one metal and does not affect the others is challenging. To simplify the process, lift off technique was employed instead of wet etching.

The contact metals for the n-GaN were Ti/Al/Ni/Au and Ni/Au for the p-GaN. Pattern generation for the lift off involved two sets of mask. The first one to be used for the n-GaN contacts only, the other one for both n-GaN and p-GaN.

Ti/Al contacts were patterned using the first set of masks. Lift off resist (LOR-5B) was spin coated for 55 secs (15 secs at 500 RPM, 40 secs at 4000 RPM) after a surface dehydration step. The sample was then soft baked at 180C for 180 secs. A thin layer of Shipley 1813 was spin coated on the LOR for 60 secs (15 secs at 500 RPM, 45 secs at 4000 RPM). The positive photoresist was soft baked at 120C for 60 secs. The photoresist was later exposed at 113 mJ/cm$^2$ and then developed using AZ 352. The developing time varied, depending on the formation of an overcut at the LOR layer.

To ensure a better adhesion of metals on the semiconductor surface, an oxygen plasma etching was done for 180 secs. Other parameters for the oxygen plasma were as follows, base pressure 40 mT, gas flow 10 sccm $O_2$ and RF power 120W. This plasma step reduced the photoresist residues that might have not gone off during the development, and provided a cleaner and better surface for the metals to adhere.

A 50 nm thin film of titanium followed by a thin layer of aluminum were deposited first using the thermal evaporator. To pattern the metals, a remover PG solution proved better than a developer. Two remover PG solution was heated to 65C on a hotplate. The dice were submerged in the first solution on the hotplate for 30 minutes. Afterwards, the dice were subjected to sonication. The sonication removed most of the unwanted metals. The dice were then put into the fresh remover PG solution for 5-10 more minutes and then rinsed in IPA and DI water.

The second set of mask was used to pattern the metals Ni/Au. Lift off resist was spin coated on the dice followed by S1813 coat following the same recipe mentioned previously. An exposure to oxygen plasma etching was also performed on dice. However, before depositing metal thin films the dice went through a diluted aluminum etchant D (contains 5-10wt% Sodium-M-Nitrobenzene Sulfonate, 55-65% Phosphoric Acid, 1-5% Acetic Acid, and 20-39% Distilled Water) for 2 minutes to remove any oxide that might have formed on the Al surface. Then a 50 nm layer of nickel was deposited using e-beam assisted metal deposition, followed by a 150 nm of gold deposition using thermal evaporation. The

unwanted metals were lifted off following the previously mentioned remover PG and sonication process.

A diagram for the fabrication process is provided below.

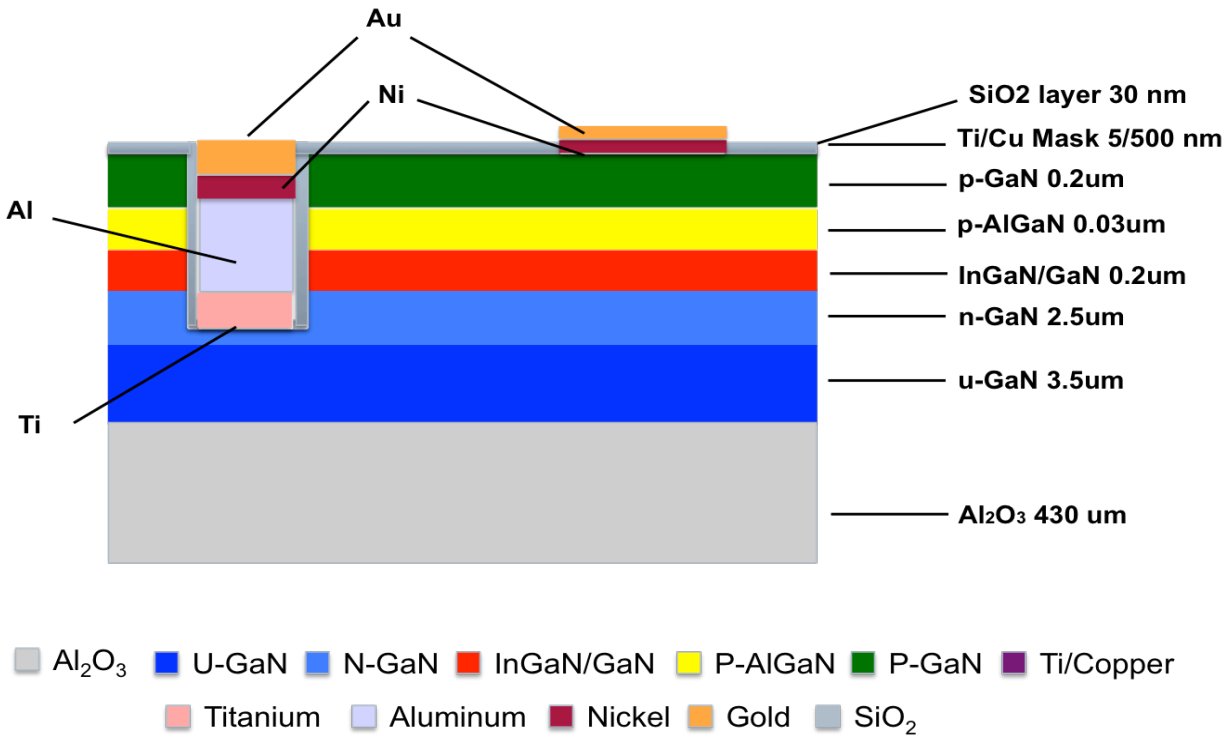


Figure 3-3. Fabrication process diagram

## 3.7 ANNEALING

In order to achieve better electrical performance, the samples were annealed in a nitrogen backflow environment. Thermal annealing was done at 150C, 300C and 450C to observe the change in both electrical and optical performance. 150C and 300C annealing was done using a high temperature oven and 450C annealing was performed in a furnace.

# CHAPTER 4: ANALYSIS

## 4.1 RIE PROCESS CHARACTERISTICS

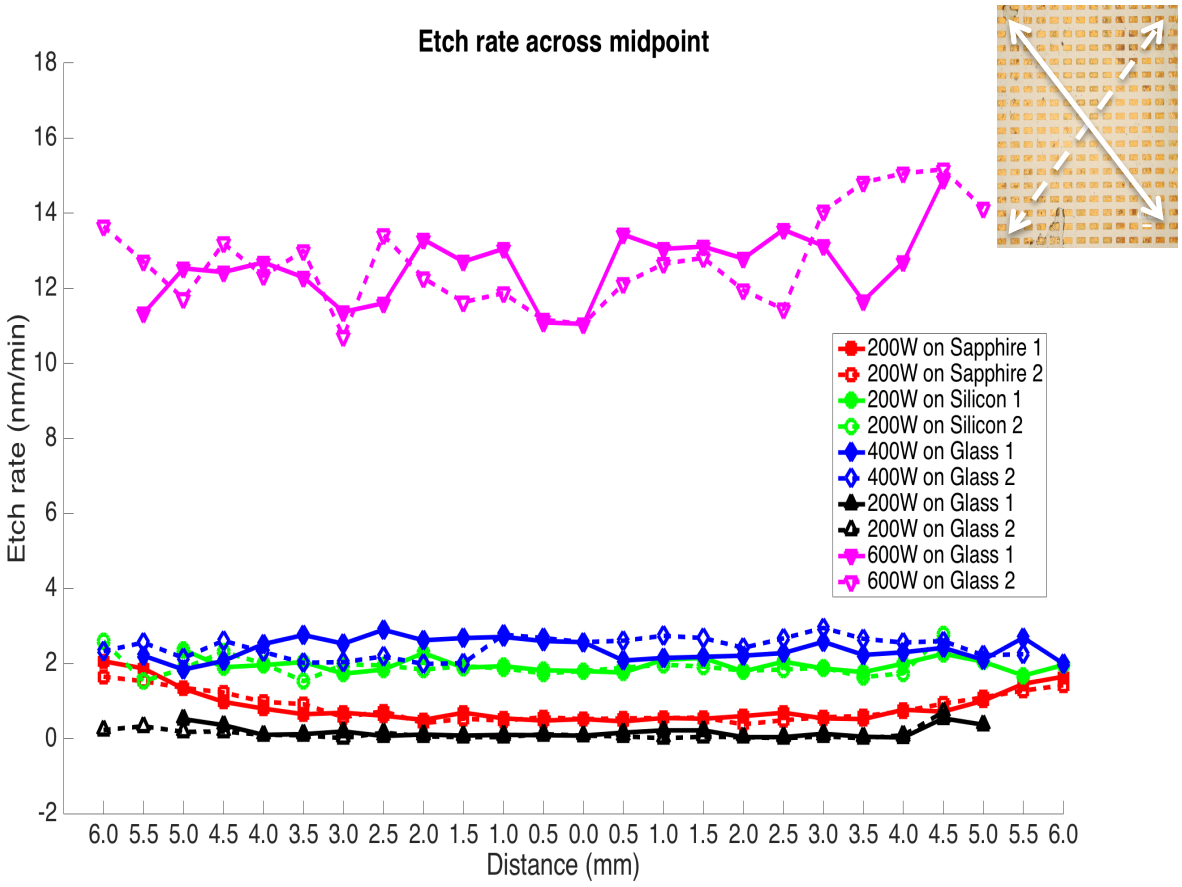


Figure 4-1. Etch rate variations measured by AFM

The etch rates were measured by atomic force microscopy indicated considerable uniformity throughout the samples. Rates were measured diagonally and presented data shows the variation from the middle of the samples to the four corners. Etch rates were found to be lowest while adding a glass substrate and highest while a silicon substrate was added. An upward change in the rates was also observed along with the increasing RF power. The changes in etch rates might be occurring due to the difference in thermal conductivity caused by different substrates.

Table 4-1. Thermal conductivity of additional substrate materials

| **Material** | **Conductivity (W/mK) @ 300K** |
|---|---|
| Sapphire | 27.21 |
| Silicon | ~149 |
| Glass | 0.8-0.9 |

The temperature during the RIE process was also investigated using temperature sensitive labels.

Table 4-2. Temperature during RIE process

| **Recipe** | **RIE Temperature (C)** |
|---|---|
| 200 W on Sapphire | 133-148 |
| 200 W on Silicon | 160-165 |
| 200 W on Glass | 149-153 |
| 400 W on Glass | 193-198 |
| 600 W on Glass | >210 |

Addition of a larger substrate than the dice might also have reduced re-deposition during the RIE process, which might have caused an increase rate for the silicon substrate added dice.

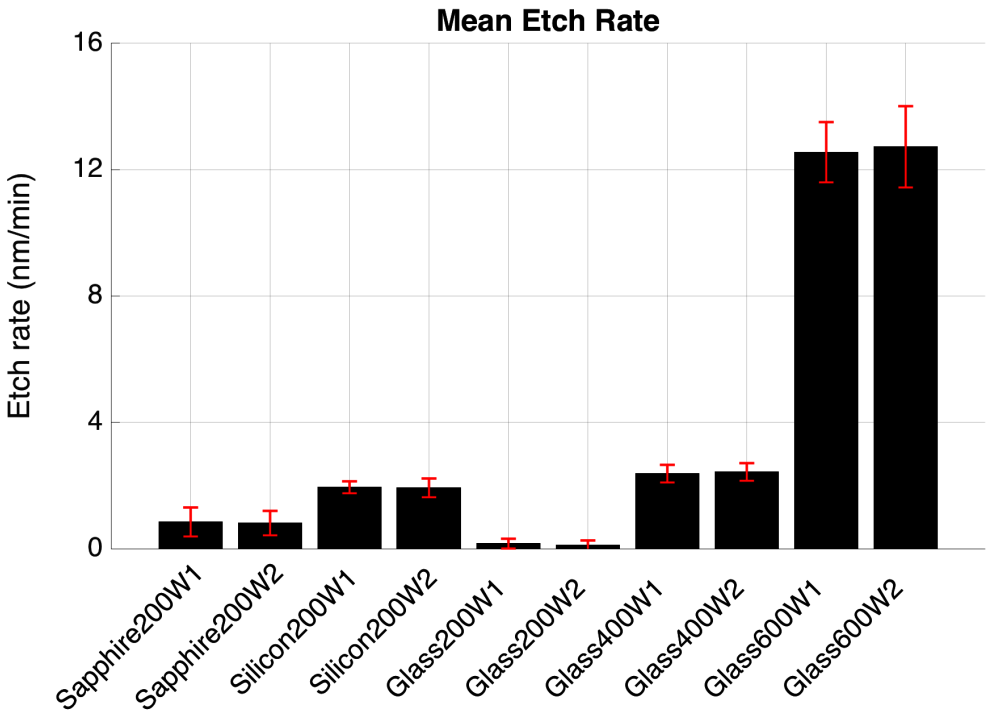


Figure 4-2. Mean etch rates for different etching recipe

Mean etch rates indicate a significant increase when 600W RF power was applied. However, the higher RF power also introduces crack and fractures on the LED's, which might be caused by the creation of pinholes and deformation in the metal mask from the high-energy ion bombardment. Surface roughness for both the RIE etched surface and the mask-covered surface was measured using atomic force microscope. The roughness of the etched surface was found to be increasing along with the increasing power. However, addition of a silicon substrate also indicated higher roughness.

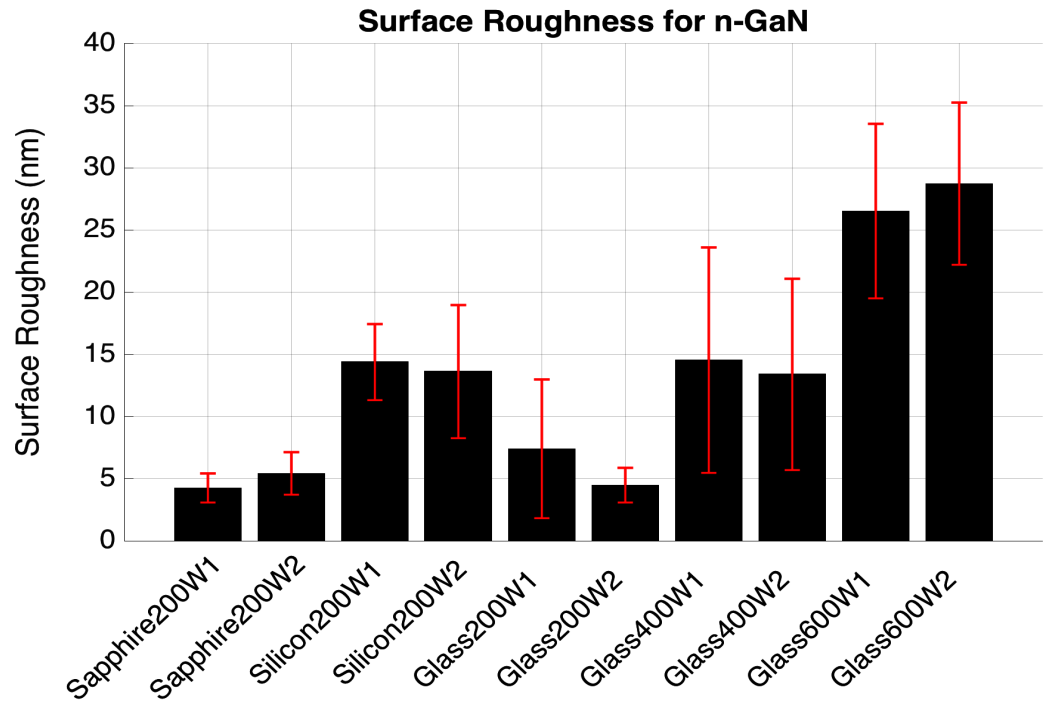


Figure 4-3. Surface roughness of n-GaN surface for different etching recipe

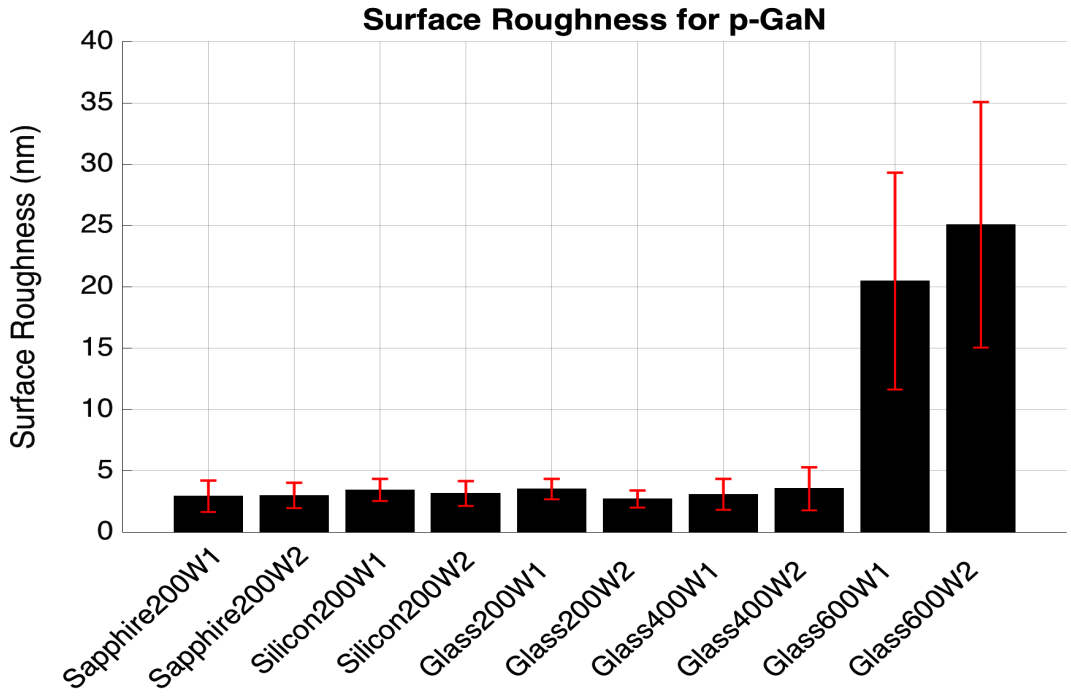


Figure 4-4. Surface roughness of p-GaN surface for different etching recipe

As mentioned before, the masked p-GaN surface indicated fairly uniform roughness except at the 600W RF power. The roughness for the masked surface might have been introduced because of the pinholes created in the mask at higher power.

Following are some AFM images of the surface roughness at different power and substrate addition.

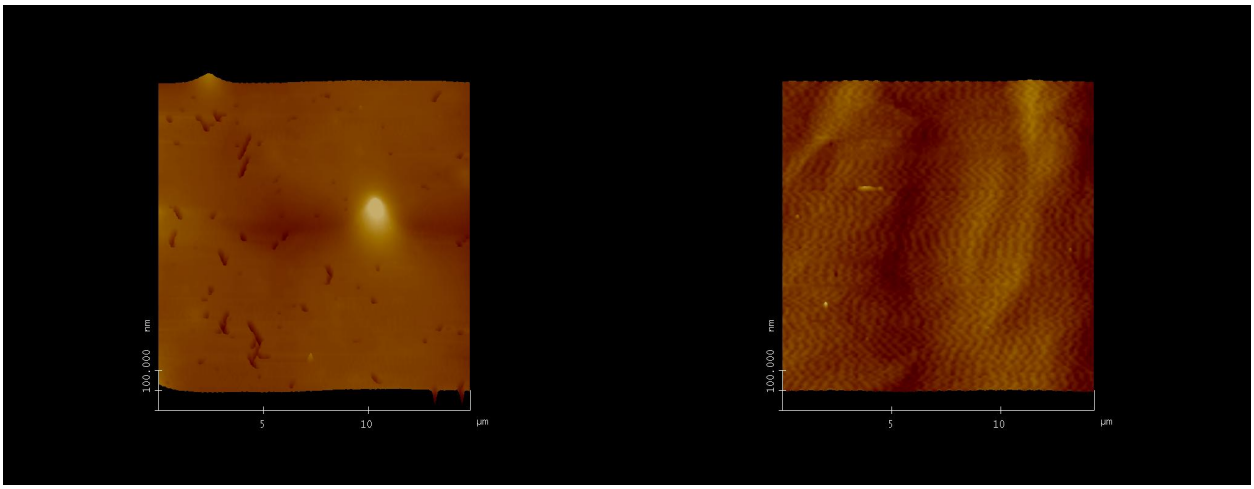


(a) (b)

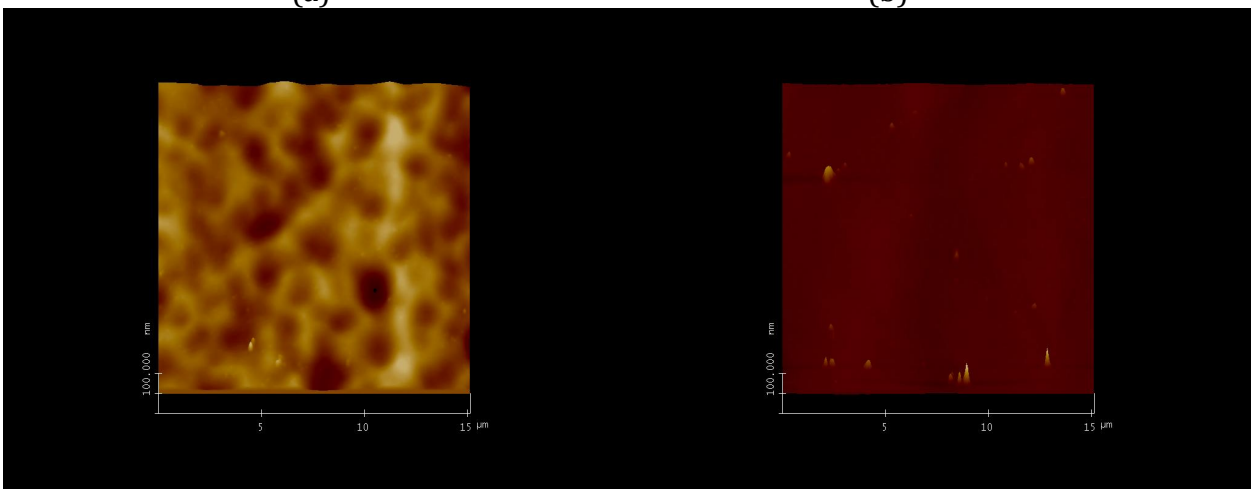


(c) (d)

Figure 4-5. Surface roughness of samples with a) 200W on sapphire n-GaN surface b) 200W on sapphire p-GaN surface c) 200W on silicon n-GaN surface d) 200W on silicon p-GaN surface e) 200W on glass n-GaN surface f) 200W on glass p-GaN surface g) 400W on glass n-GaN surface h) 400W on glass p-GaN surface i) 600W on glass n-GaN surface j) 600W on glass p-GaN surface

Figure 4-5 (Cont'd)

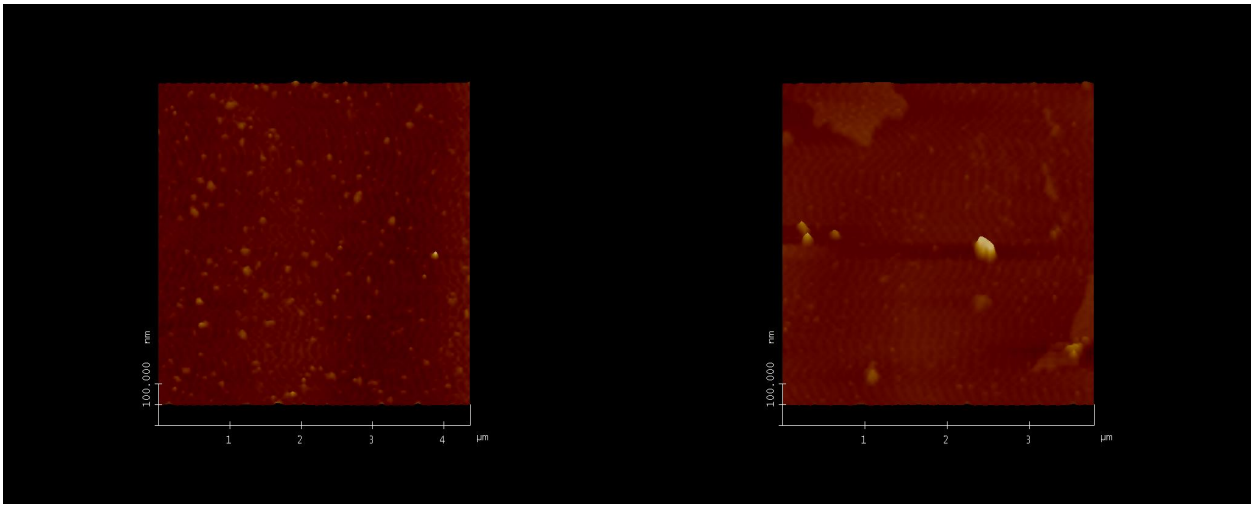


(e)




(f)

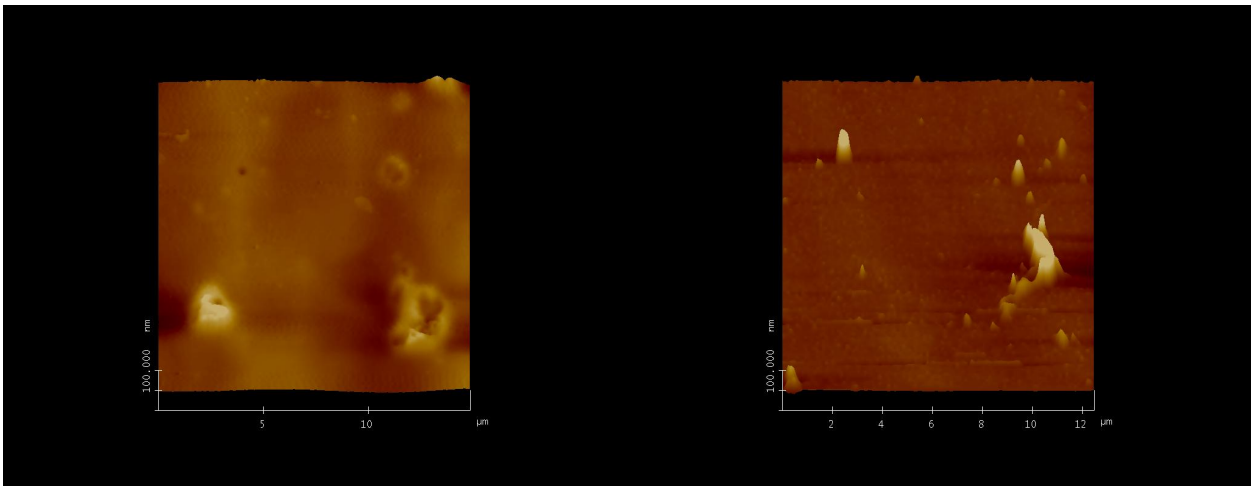


(g)




(h)

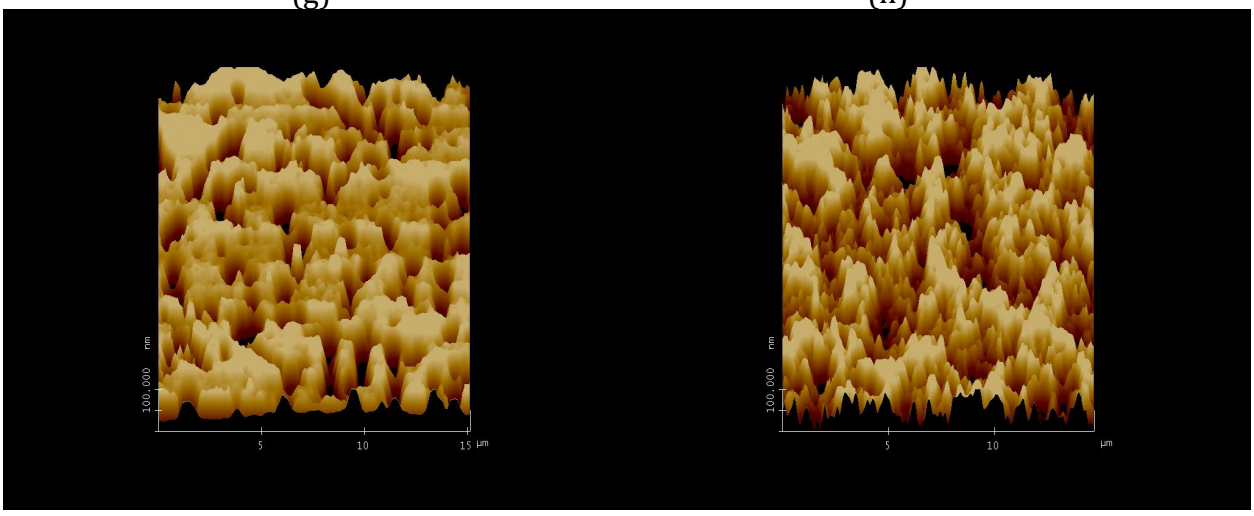


(i)




(j)

## 4.2 ELECTRICAL PROPERTIES

The current voltage relationships were characterized for the samples with a sapphire substrate and a silicon substrate addition etched at 200W RF power.

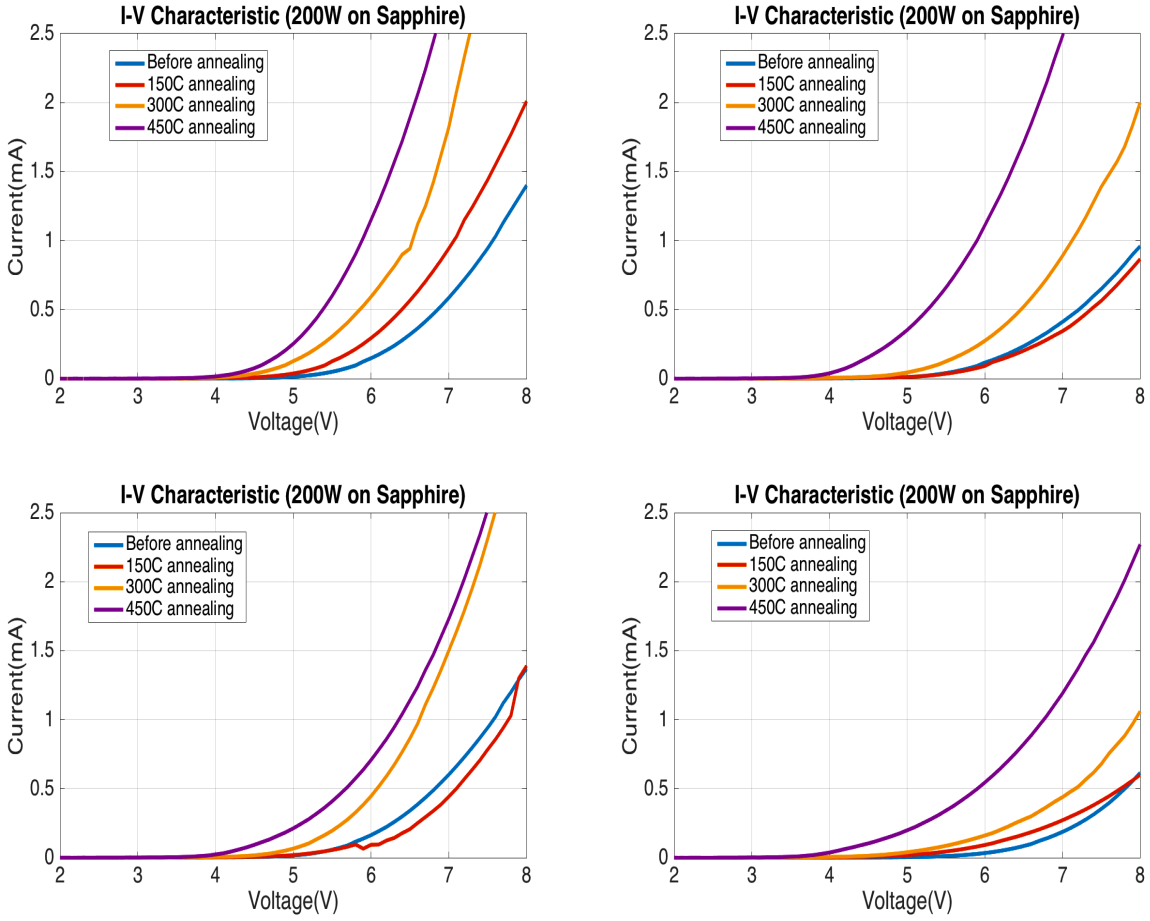


Figure 4-6. I-V characteristics of LED's etched at 200W on sapphire substrate

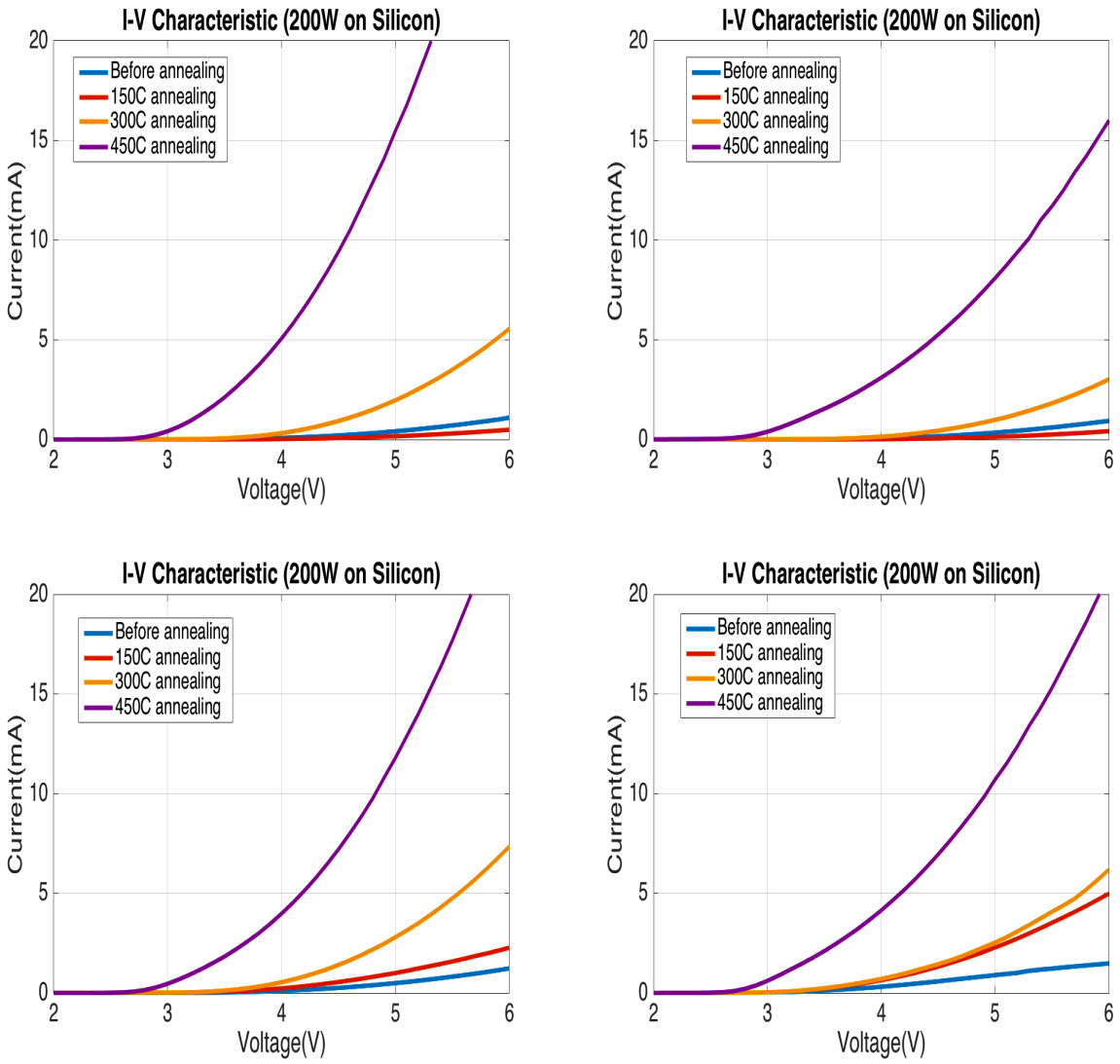


Figure 4-7. I-V characteristics of LED's etched at 200W on silicon substrate

The I-V characteristics indicate that with annealing at higher temperatures, current carrying capacity increases for the same applied voltage. Also, the turn-on voltage for the LED decreases with the increasing annealing temperature.

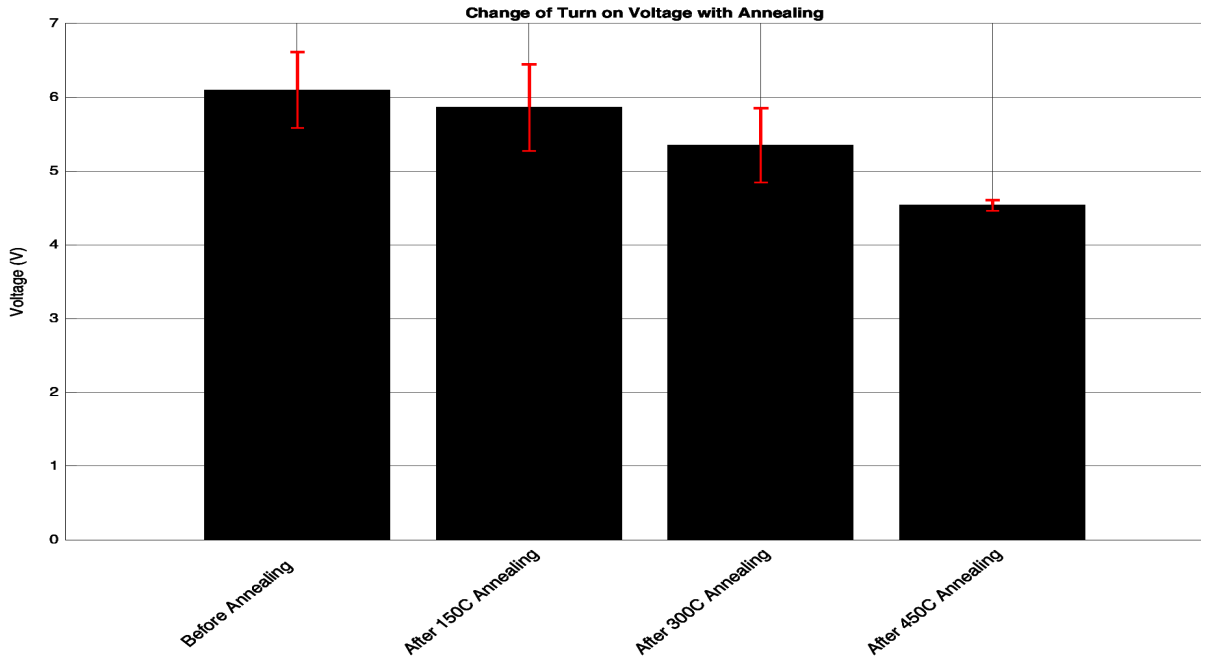


Figure 4-8. Change in turn-on voltage (etched at 200W on sapphire substrate)

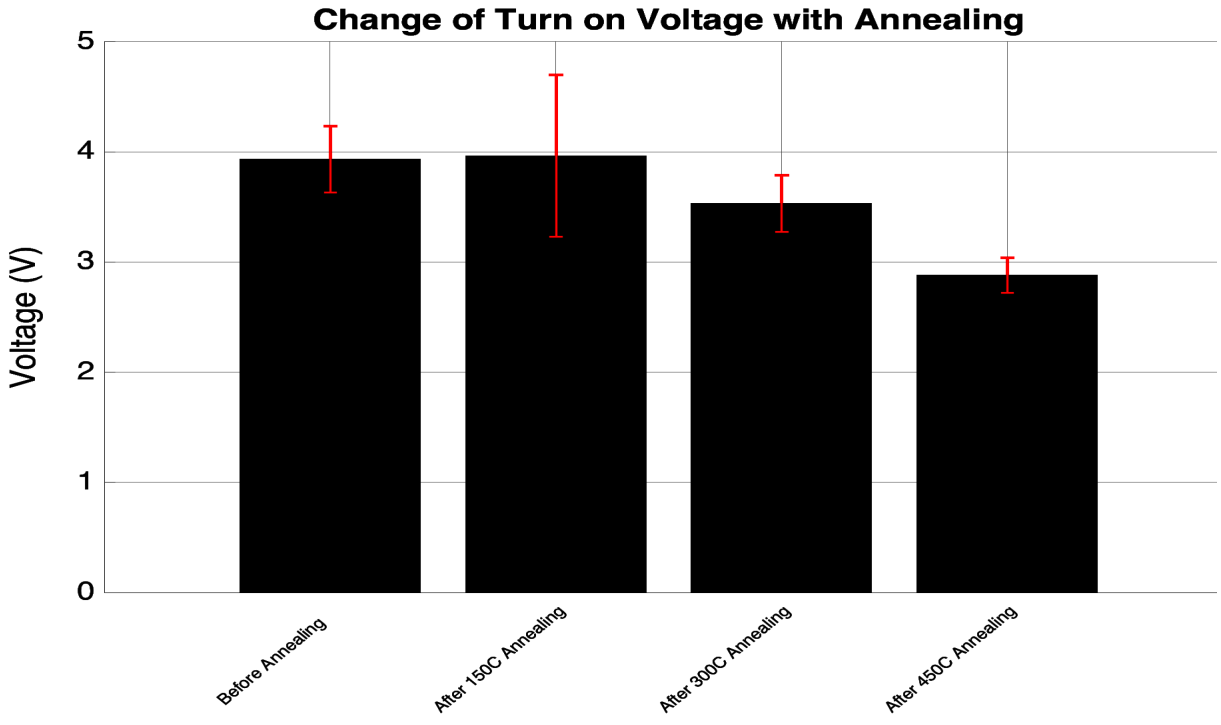


Figure 4-9. Change in turn-on voltage (etched at 200W on silicon substrate)

The annealing causes a decrease in the resistance of the LED's, which might be the primary reason behind these phenomena.

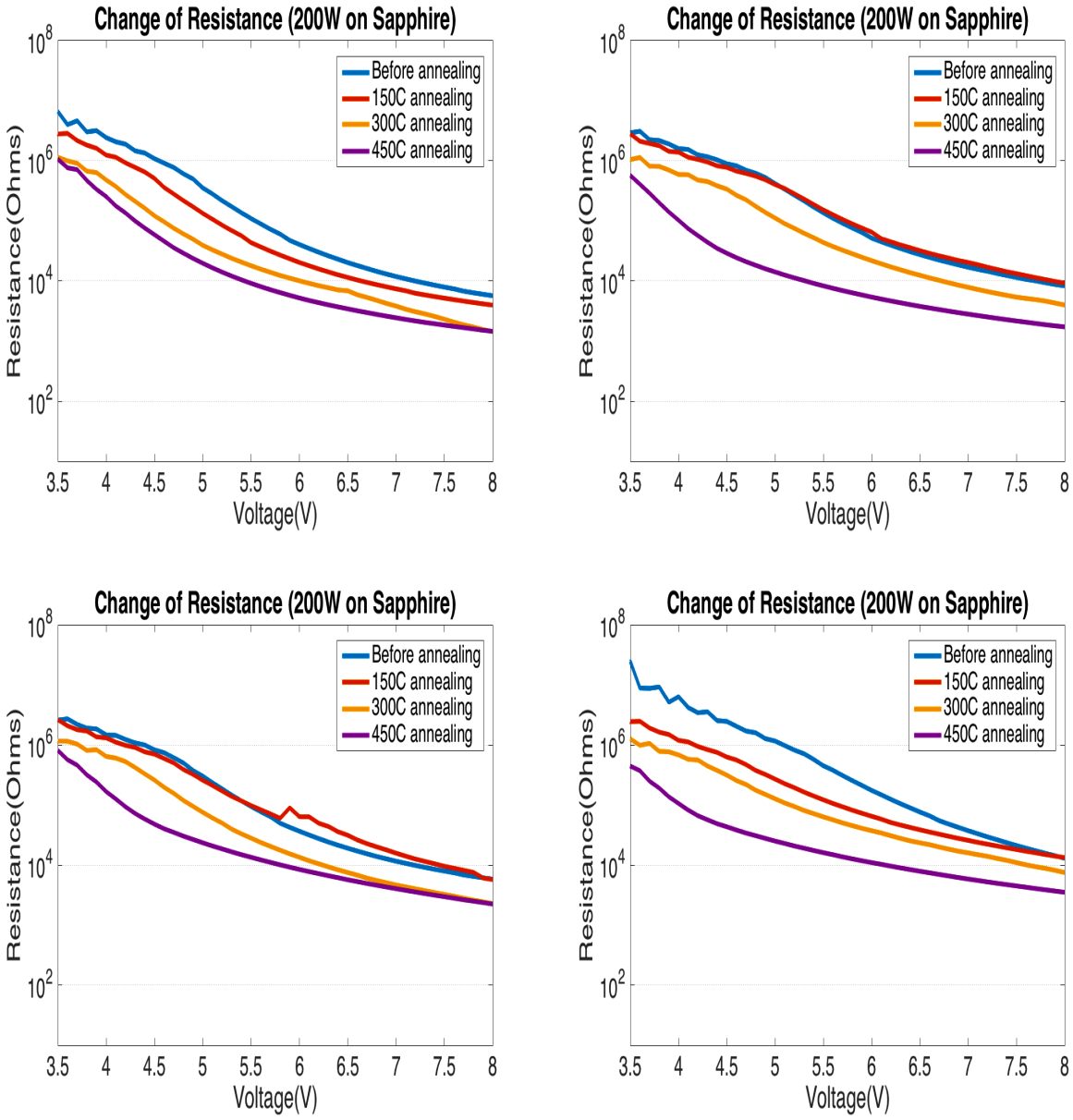


Figure 4-10. Change in resistance for LED's at 200W on sapphire substrate

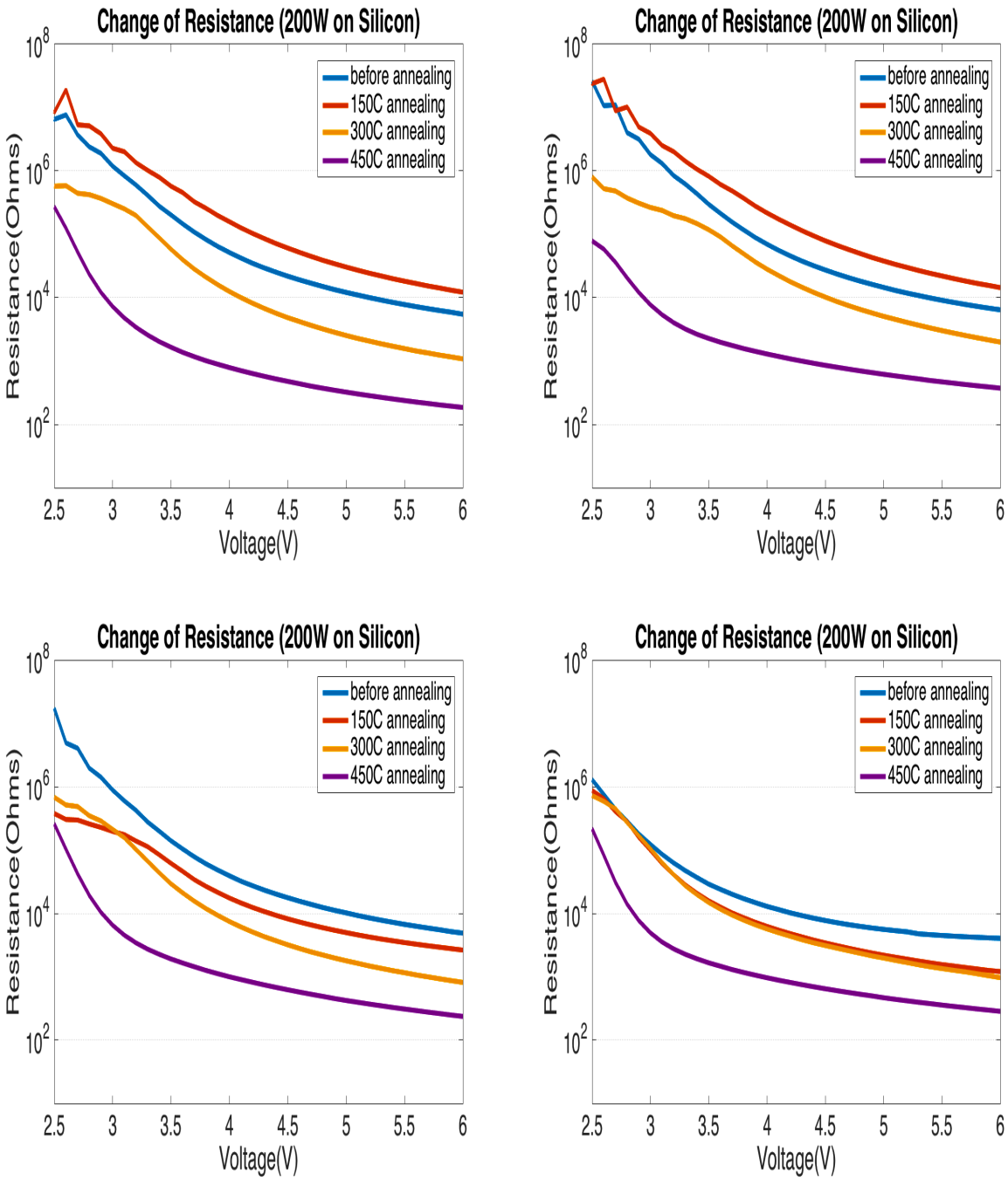


Figure 4-11. Change in resistance for LED's at 200W on silicon substrate

## 4.3 OPTICAL PROPERTIES

The light intensity improved with subsequent annealing steps. As the resistance was decreasing with annealing temperature rise, lower energy loss occurred which might have caused a rise in light intensity.

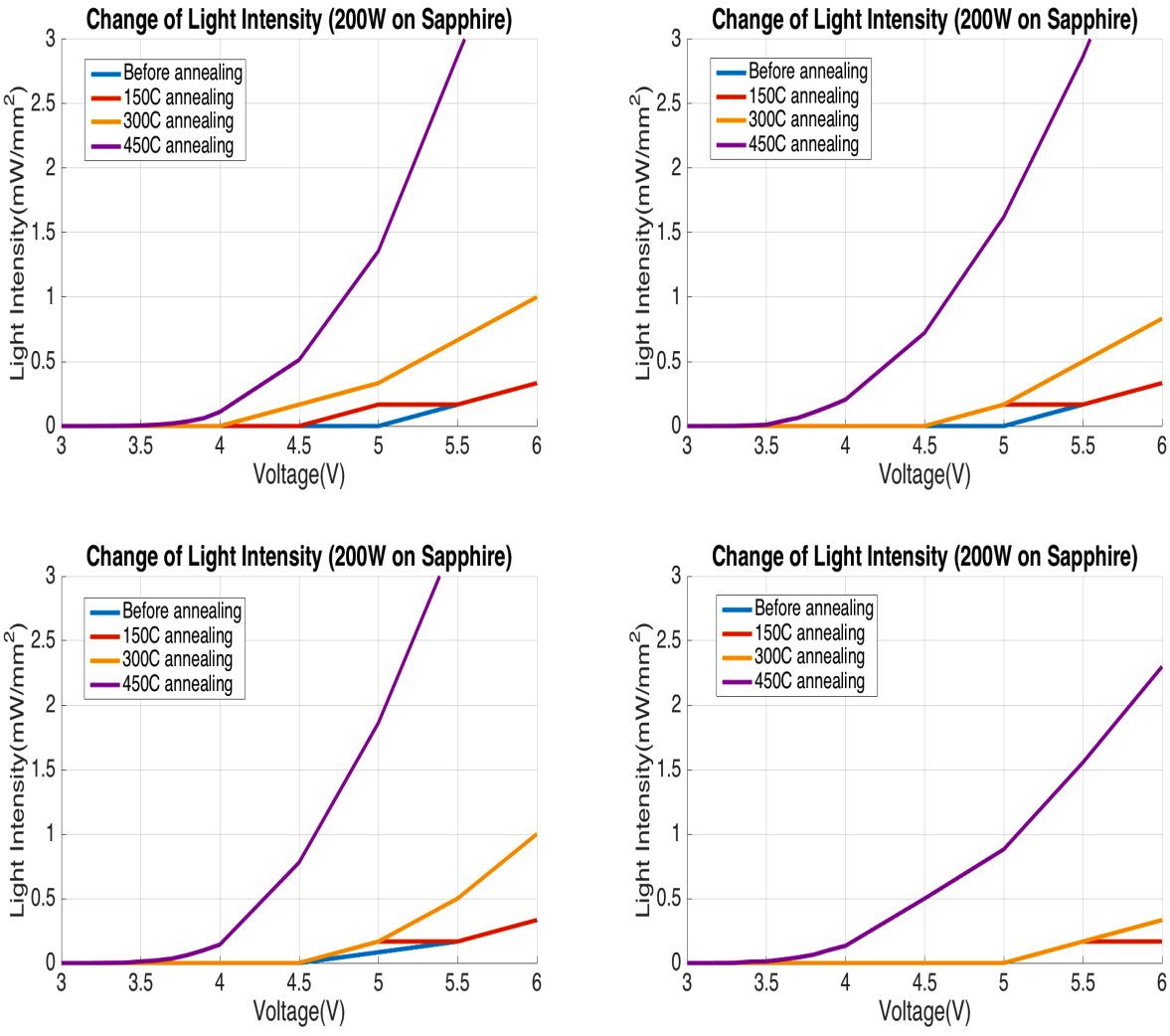


Figure 4-12. Change in light intensity for LED's at 200W on sapphire substrate

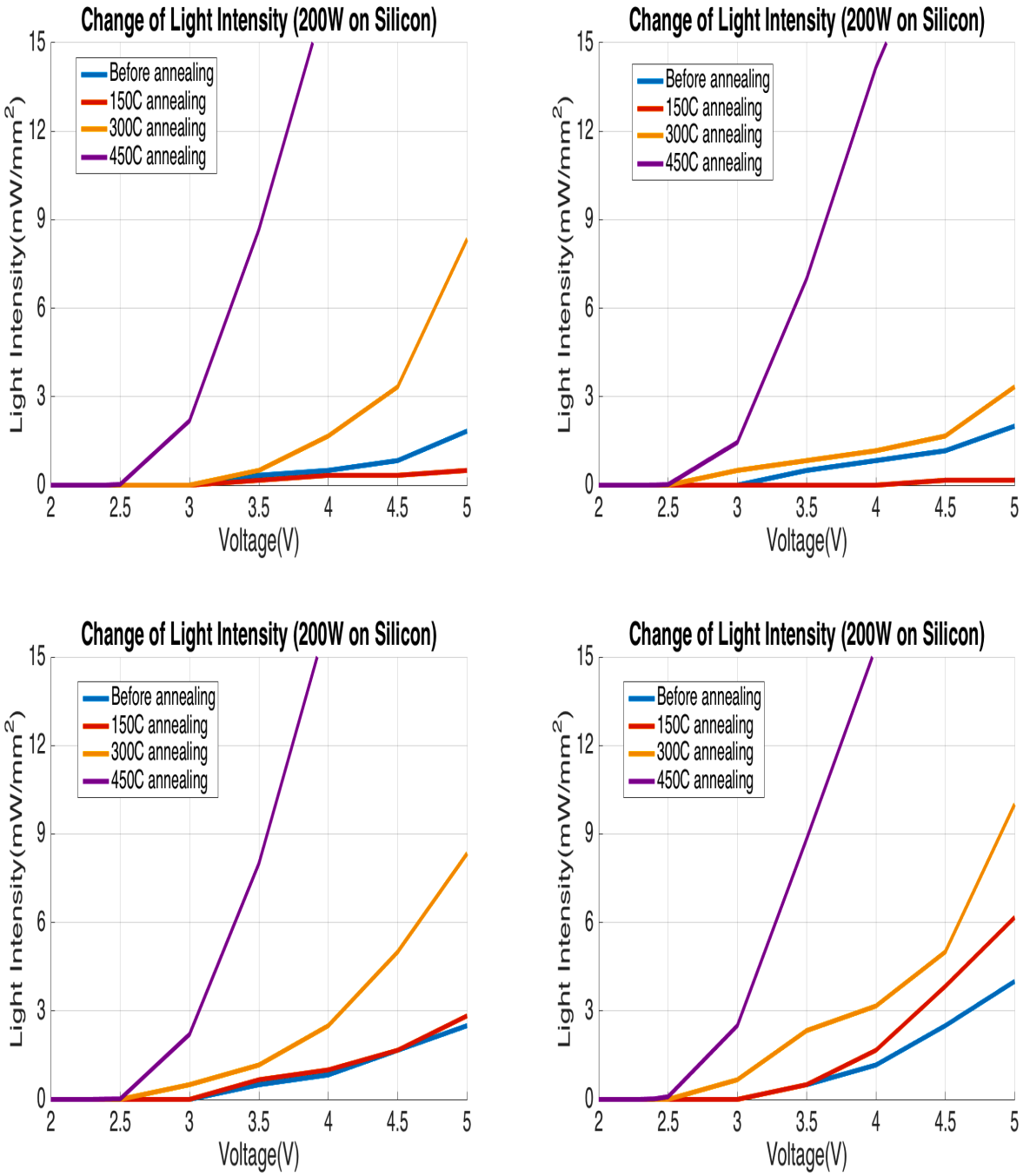


Figure 4-13. Change in light intensity for LED's at 200W on silicon substrate

## 4.4 THERMAL PROPERTIES

While performing optogenetics experiments in vivo, heat will accumulate in the LED's. The figures below plot the temperature rise at the surface of the LED's (measured by infrared camera) as a function of increasing input electrical power. While the sample on sapphire exceeds the limit of 2C [48] at elevated power levels, the silicon sample remains below the limit even at higher power.

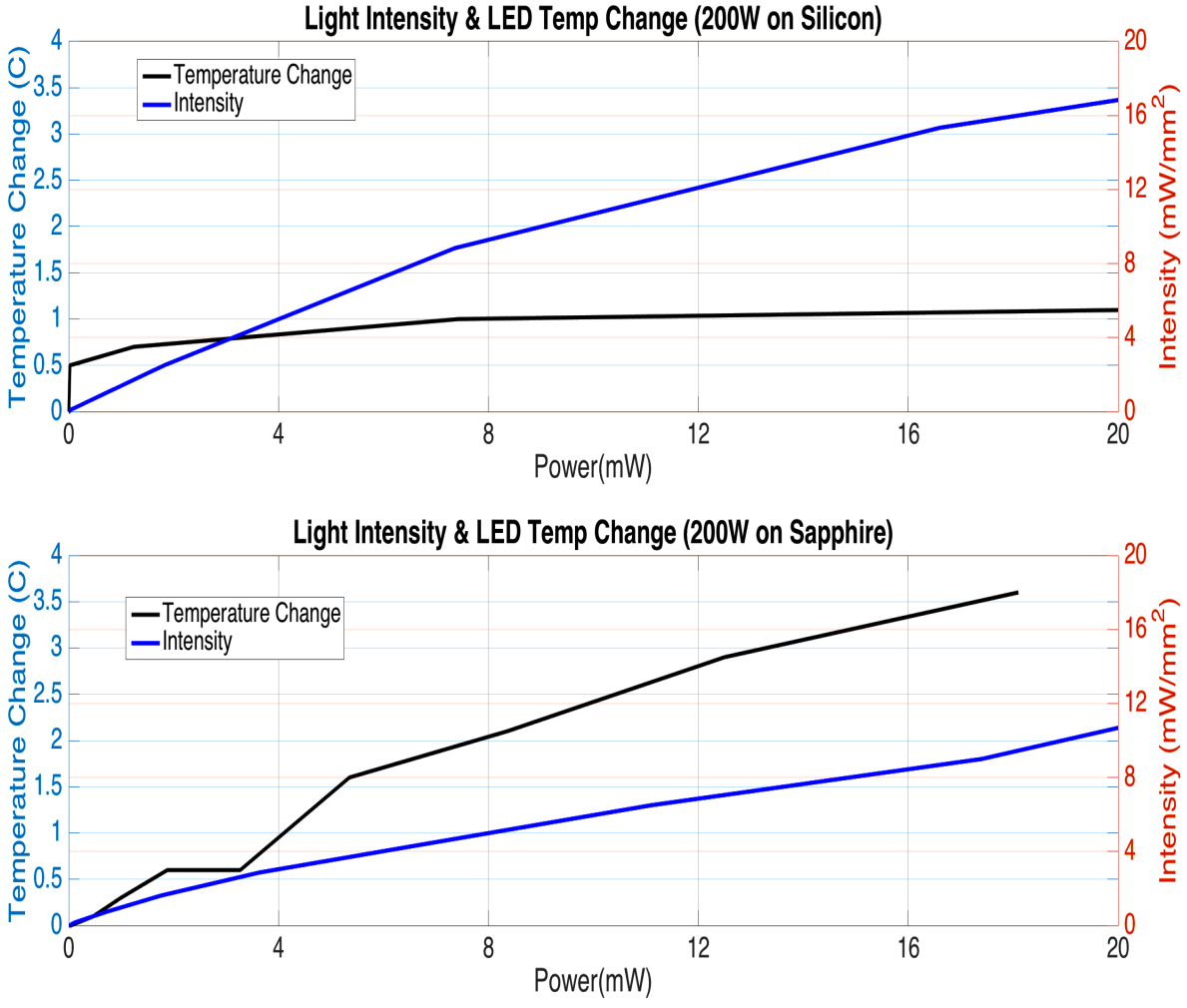


Figure 4-14. Temp and Intensity change with electrical power

# CHAPTER 5: CONCLUSION AND OUTLOOK

This thesis has discussed the fabrication process and characterization of monolithic multichannel GaN LED arrays for use in optogenetics. The fabrication process incorporates the etching of GaN using conventional reactive ion etching process, which is less expensive than other commonly used etching process like ICP-RIE. Monolithic fabrication will allow integration of other techniques like metal interconnects, micro lenses, waveguides on the LED's and therefore simplifying the process. This approach will also make the process labor, time and cost efficient. Furthermore, the multichannel stimulation will be able to provide site-specific stimulation over a wide region of interest on the cortex. The arrays demonstrate the light intensity necessary for optogenetics purposes. The temperature rise was also found to be within the acceptable range for one of the working arrays. These properties meet the key performance requirements for optogenetics. Despite having met the goals, some work still remains. A complete stimulation and recording device could be made out of these arrays by incorporating recording electrodes. A flexible device could also be made possible using the arrays by transferring them on a flexible substrate such as PET.

One drawback of these arrays – they still have a higher resistance. This resistance might be reduced by further higher annealing. Reducing the resistance will lower the loss in heat dissipation, and subsequently might increase the light intensity.

# BIBLIOGRAPHY

# BIBLIOGRAPHY


1. Karl Desseiroth, "Optogenetics: 10 years of microbial opsins in neuroscience", *nature neuroscience*, volume 18, vol 9, 2015

2. Ofer Yizhar, Lief E. Fenno, Thomas J. Davidson, Murtaza Mogri, Karl Deisseroth, "Optogenetics in Neural Systems", *Neuron,* vol 71, 2011, Elsevier Inc.

3. Karl Deisseroth, "Optogenetics", *nature methods*, Vol 8 , 2011.

4. Boyden, E.S., Zhang, F., Bamberg, E., Nagel, G. & Deisseroth, K. *Nat. Neurosci*. 8, 1263–1268, 2005.

5. Oesterhelt, D. & Stoeckenius, W., *Nat. New Biol.* 233, 149–152, 1971.

6. Matsuno-Yagi, A. & Mukohata, Y., *Biochem. Biophys. Res. Commun.*, 78, 237–243, 1977.

7. Nagel, G. et al. *Science* 296, 2395–2398, 2002.

8. Racker, E., and Stoeckenius, W., "Reconstitution of purple membrane vesicles catalyzing light-driven proton uptake and adenosine triphosphate formation", *J. Biol. Chem*. 249, 662–663, 1974.

9. Essen, L.O., "Halorhodopsin: light-driven ion pumping made simple?" *Curr. Opin. Struct. Biol.* 12, 516–522, 2002.

10. Nagel, G., Ollig, D., Fuhrmann, M., Kateriya, S., Musti, A.M., Bamberg, E., and Hegemann, P., "Channelrhodopsin-1: a light-gated proton channel in green algae", *Science* 296, 2395–2398, 2002.

11. Boyden, E.S., Zhang, F., Bamberg, E., Nagel, G., and Deisseroth, K., "Millisecond-timescale, genetically targeted optical control of neural activity", *Nat. Neurosci.* 8, 1263–1268, 2005.

12. Gradinaru, V., Zhang, F., Ramakrishnan, C., Mattis, J., Prakash, R., Diester, I., Goshen, I., Thompson, K.R., and Deisseroth, K., "Molecular and cellular approaches for diversifying and extending optogenetics" *Cell* 141, 154–165, 2010.

13. Chow, B.Y., Han, X., Dobry, A.S., Qian, X., Chuong, A.S., Li, M., Henninger, M.A., Belfort, G.M., Lin, Y., Monahan, P.E., and Boyden, E.S. "High-performance genetically targetable optical neural silencing by light-driven proton pumps". *Nature* 463, 98–102, 2010.

14. Cardin J. A., Carlén M., Meletis K., Knoblic U., Zhang F., Deisseroth K., Li-Huei Tsai, Moore C. I., "Driving fast-spiking cells induces gamma rhythm and controls sensory responses", *Nature* 459, 663-667, 2009.

15. Alexander M Aravanis, Li-PingWang, Feng Zhang, Leslie A Meltzer, MurtazaZMogri, M Bret Schneider and Karl Deisseroth, "An optical neural interface: in vivo control of rodent motor cortex with integrated fiberoptic and optogenetic technology", *J. Neural Eng.* 4, S143–S156, 2007.

16. C. R. Eddy, Jr., *MRS Internet J. Nitride Semicond. Res*., 4S1, G10.5, 1999.

17. R. J. Shul, "GaN and Related Materials", edited by S. J. Pearton, Gordon and Breach, New York, 1997.

18. Mileham J R, Pearton S J, Abernathy C R, Mackenzie J D, Shul R J and Kilcoyne S P, *J. Vac. Sci. Technol*. A 14 836, 1996.

19. Pankove J I, *J. Electrochem. Soc.*, 119 1118, 1992.

20. R. Cheung, R. J. Reeves, B. Rong, S. A. Brown, E. J. M. Fakkeldij, E. van der Drift, and M. Kamp, *J. Vac. Sci. Technol*. B 17, 2759, 1999.

21. D Basak, M Verd, M T Montojo, M A S´anchez-Garc´ıa, F J S´anchez, E Mu˜noz and E Calleja, "Reactive ion etching of GaN layers using SF6", *Semicond. Sci. Technol.*, 12, 1654–1657, 1997.

22. Pearton S J, Abernathy C R, Vartuli C B, Mackenzie J D, Shul R J, Wilson R G and Zavada J M, *Electron. Lett.* 31, 836, 1995.

23. Shul R J, Kilcoyne S P, Craeford M H, Parmeter J E, Vartuli C B, Abernathy C R and Pearton S J, *Appl. Phys. Lett.*, 66, 1761, 1995.

24. Ping A T, Adesida I, Asif Khan M and Kuznia J N, *Electron. Lett.,* 30, 1895, 1994.

25. Humphreys B and Govett M, *Mater. Res. Soc. Internet J. Nitride Semicond. Res.,* 1, 28, 1997.

26. S. J. Pearton, R. J. Shul, and F. Ren, *MRS Internet J. Nitride Semicond. Res.*, 5, 11, 2000.

27. Y. H. Lee, Y. J. Sung, G. Y. Yeom, J. W. Lee, and T. I. Kim, *J. Vac. Sci. Technol.*, A 18, 1390, 2000.

28. I. Adesida, C. Youtsey, A. T. Ping, F. Khan, L. T. Romano, and G. Bulman, *MRS Internet J. Nitride Semicond. Res.*, 4S1, G1.4, 1999.

29. A. P. Zhang, G. Dang, F. Ren, X. A. Cao, H. Cho, E. S. Lambers, S. J. Pearton, R. J. Shul, L. Zhang, A. G. Baca, R. Hickman, and J. M. Van Hove, *MRS Internet J. Nitride Semicond. Res.*, 5S1, W11.66, 2000.

30. J. Lee, H. Cho, D. C. Hays, C. R. Abernathy, S. J. Pearton, R. H. Shul, G. A. Vawter, and J. Han, *IEEE J. Sel. Top. Quantum Electron*, 4, 557, 1998.

31. A. T. Ping, I. Adesida, and M. A. Khan, *Appl. Phys. Lett.*, 67, 1250, 1995.

32. F. Binet, J. Y. Duboz, N. Laurent, C. Bonnat, P. Collot, F. Hanauer, O. Briot, and R. L. Aulombard, *Appl. Phys. Lett.*, 72, 960, 1998.

33. M. Kneissl, D. P. Bour, N. M. Johnson, L. T. Romano, B. S. Krusor, R. Donaldson, J. Walker, and C. Dunnrowicz, *Appl. Phys. Lett.,* 72, 1539, 1998.

34. T. Shen, G. Gao, and H. Morkoc, "Recent developments in ohmic contacts for III–V compound semiconductors," *J. Vac. Sci. Technol. B, Microelectron.*, vol. 10, no. 5, pp. 2113–2132, 1992.

35. Y. Koide, H. Ishikawa, S. Kobayashi, S. Yamasaki, S. Nagai, J. Umezaki, M. Koike, and M. Murakami, "Dependence of electrical properties on work functions of metals contacting to p-type GaN," *Appl. Surf. Sci*., vol. 117/118, no. 2, pp. 373–379, 1997.

36. J. S. Foresi and T. D. Moustakas, "Metal contacts to gallium nitride," *Appl. Phys. Lett.*, vol. 62, no. 22, pp. 2859–2861, 1993.

37. M. E. Lin, Z. Ma, F. Y. Huang, Z. F. Fan, L. H. Allen, and H. Morkoc, "Low resistance ohmic contacts on wide band-gap GaN," *Appl. Phys. Lett.*, vol. 64, no. 8, pp. 1003–1005, 1994.

38. J. O. Song, S.-J. Park, and T.-Y. Seong, "Effects of sulfur passivation on Ti/Al ohmic contacts to n-type GaN using CH3CSNH2 solution," *Appl. Phys. Lett.*, vol. 80, no. 17, pp. 3129–3131, 2002.

39. S. Ruvimov, Z. Liliental-Weber, J.Washburn, K. J. Duxstad, E. E. Haller, Z. Fan, S. Mohammad, W. Kim, A. E. Botchkarev, and H. Morkoc, "Microstructure of Ti/Al and Ti/Al/Ni/Au ohmic contacts for n-GaN," *Appl. Phys. Lett.*, vol. 69, no. 11, pp. 1556–1558, 1996.

40. C. M. Pelto, Y. Chang, Y. Chen, and R. S. Williams, "Thermally stable, oxidation resistant capping technology for Ti/Al ohmic contact contacts to n-GaN," *Appl. Phys. Lett.*, vol. 92, no. 8, pp. 4283–4285, 2002.

41. A. Motayed, K. Jones, M. A. Derenge, M. C. Wood, D. Zakharov, Z. Liliental-Weber, A. V. Davydov, W. T. Anderson, A. A. Iliadis, and S. Mohammad, "Electrical,

microstructural, and thermal stability characteristics of Ta/Ti/Ni/Au contacts to n-GaN," *J. Appl. Phys.*, vol. 95, no. 3, pp. 1516–1524, 2004

42. J. O. Song, S.-H. Kim, J. Kwak, and T.-Y. Seong, "Formation of V-based ohmic contacts to n-GaN," *Appl. Phys. Lett.*, vol. 83, no. 6, pp. 1154– 1156, 2003.

43. J. T. Trexler, S. J. Pearton, P. H. Holloway, M. G. Mier, K. R. Evans, and R. F. Karlicek, "Comparison of Ni/Au, Pd/Au, Cr/Au metallizations for ohmic contacts to p-GaN," *Proc. Mater. Res. Symp.*, vol. 449, pp. 1091–1094, 1997.

44. Jung-Hun Seo, Jing Li, Jaeseong Lee, Shaoqin Gong, Jingyu Lin, Hongxing Jiang, Zhenqiang Ma, "A Simplified Method of Making Flexible Blue LEDs on a Plastic Substrate", *IEEE Photonics Journal*, Vol. 7, No. 2, 2015.

45. N. A. Papanicolaou, M. V. Rao, J. Mittereder, W. T. Anderson, "Reliable Ti/Al and Ti/Al/Ni/Au ohmic contacts to n-type GaN formed by vacuum annealing", *J. Vac. Sci. Technol*. B 19.1, 2001.

46. M. E. Lin, Z. Ma, F. Y. Huang, Z. F. Fan, L. H. Allen, and H. Morkoc¸, *Appl. Phys. Lett*., 64, 1003, 1994

47. Z. Fan, S. N. Mohammed, W. Kim, O. Aktas, A. E. Botchkarev, K.Duxstad, and E. E. Haller, *J. Electron. Mater*. 25, 1703, 1996.

48. Niall McAlinden, David Massoubre, Elliot Richardson, Erdan Gu, Shuzo Sakata, Martin D. Dawson and Keith Mathieson, "Thermal and optical characterization of micro-LED probes for in vivo optogenetic neural stimulation", *Optics Letters*, Vol. 38, No. 6, 2013.